

Advanced Processing of Hyperspectral Images

State of Science of Environmental Applications of Imaging Spectroscopy
in honor of Dr. Alexander F.H. Goetz

A. Plaza¹, J. A. Benediktsson², J. Boardman³, J. Brazile⁴, L. Bruzzone⁵, G. Camps-Valls⁶,
J. Chanussot⁷, M. Fauvel^{2,7}, P. Gamba⁸, A. Gualtieri^{9,10}, M. Marconcini⁵, J. C. Tilton⁹, G. Trianni⁸

¹Univ. Extremadura (Spain), ²University of Iceland, ³Analytical Imaging and Geophysics LLC (USA),

⁴Univ. Zürich (Switzerland), ⁵Univ. Trento (Italy), ⁶Univ. Valencia (Spain), ⁷INPG Grenoble (France),

⁸Univ. Pavia (Italy), ⁹NASA/Goddard Space Flight Center (USA), ¹⁰Global Science & Technology (USA)

Talk Outline

1. Introduction

2. Classification of hyperspectral images using kernel methods

- Composite kernels
- Transductive SVMs

3. Integration of spatial and spectral information

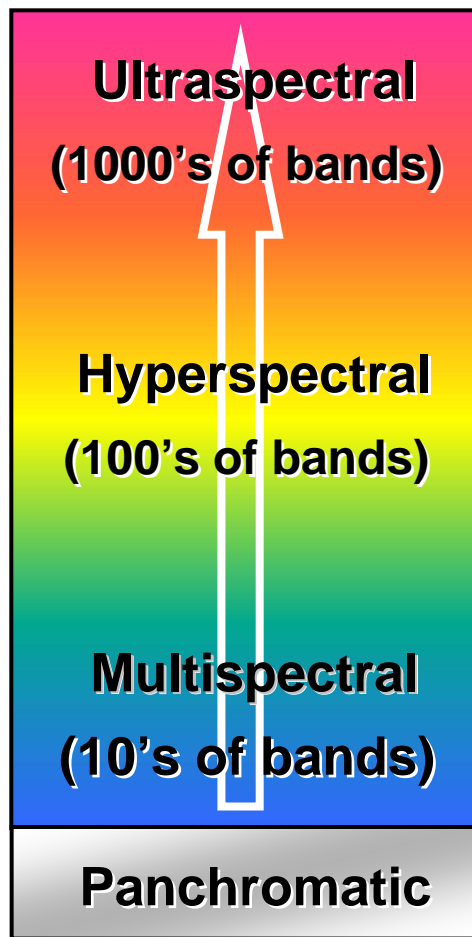
- Mathematical morphology-based approaches
- Spatial/spectral endmember extraction and spectral unmixing
- Markov random fields (MRF)
- Hierarchical segmentation

4. Parallel implementations

5. Experimental results

6. Conclusions

Levels of Spectral Information in Remote Sensing



Spectral mixture analysis: Determines the abundance of materials (e.g. precision agriculture).

Characterization: Determines variability of identified material (e.g. wet/dry sand, soil particle size effects).

Identification: Determines the unique identity of the foregoing generic categories (e.g. land-cover or mineral mapping).

Discrimination: Determines generic categories of the foregoing classes.

Classification: Separates materials into spectrally similar groups (e.g., urban data classification).

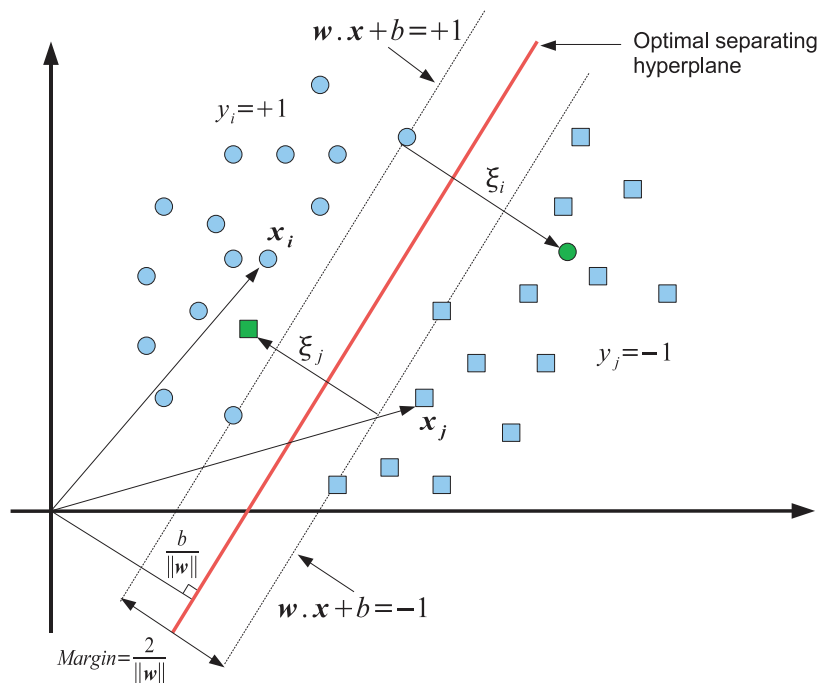
Detection: Determines the presence of materials, objects, activities, or events.

Challenges in hyperspectral image processing

- The special characteristics of hyperspectral data pose several *processing problems*:
 1. The high-dimensional nature of hyperspectral data introduces important limitations in supervised classifiers, such as the **limited availability of training samples** or the inherently complex structure of the data.
 2. There is a need to **integrate the spatial and spectral information** to take advantage of the complementarities that both sources of information can provide, in particular, for unsupervised data processing.
 3. There is a need to develop **parallel algorithm implementations**, able to speed up algorithm performance and to satisfy the extremely high computational requirements of time-critical remote sensing applications.
- In this work, we have taken a necessary first step towards the understanding and assimilation of the above aspects in the design of *last-generation hyperspectral image processing algorithms*.

Support Vector Machines (SVMs)

- High-dimensional spaces are mostly *empty*, making density estimation difficult.
- SVMs consider *geometrical* rather than *statistical* properties of the classes.
 - ✓ *Kernel-trick* allows one to work in the *mapped* kernel space.
 - ✓ No need to know the *mapping function*: $\langle \Phi(\mathbf{x}_i), \Phi(\mathbf{x}_j) \rangle = k(\mathbf{x}_i, \mathbf{x}_j)$



Polynomial kernel:

$$k_{poly}(\mathbf{x}, \mathbf{z}) = (\langle \mathbf{x}, \mathbf{z} \rangle + \theta)^d$$

SAM kernel:

$$k_{SAM}(\mathbf{x}, \mathbf{z}) = \exp(-\gamma \alpha(\mathbf{x}, \mathbf{z})^2)$$

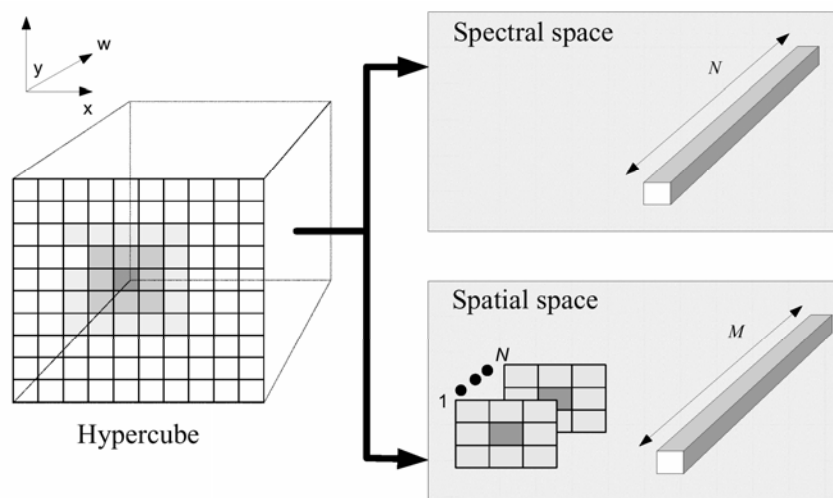
$$\alpha(\mathbf{x}, \mathbf{z}) = \arccos\left(\frac{\langle \mathbf{x}, \mathbf{z} \rangle}{\|\mathbf{x}\| \cdot \|\mathbf{z}\|}\right)$$

Gaussian RBF kernel:

$$k_{gauss}(\mathbf{x}, \mathbf{z}) = \exp(-\gamma \|\mathbf{x} - \mathbf{z}\|^2)$$

Composite Kernels for Image Classification

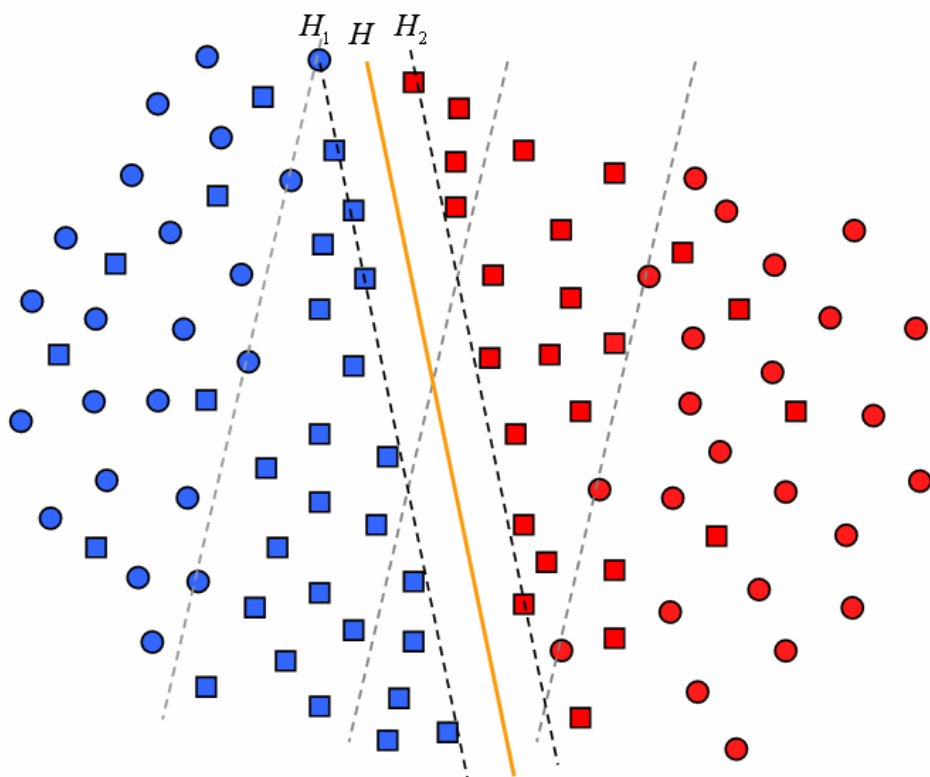
- *Some Properties of Mercer's kernels:*
 - ✓ Sum of valid kernels *is* a valid kernel.
 - ✓ Scaling a valid kernel by a positive factor *is* a valid kernel
 - ✓ Tensor product of valid kernels *is* a valid kernel.
- From *Functional Analysis*, the direct sum of Hilbert spaces allows elegant integration of different information sources in any *kernel* machine.
- To decompose the *spectral* and *contextual/ spatial* information and *merge it in the composite kernel*.
- New family of composite kernels developed, accounting for *spatial*, *spectral* and cross-information simultaneously.



Transductive Support Vector Machines (TSVMs)

- Based on the joint use of *labeled* and *unlabeled* patterns in the framework of a *transductive iterative learning process*.

Standard Inductive Approach: The learning of the classifier is carried out only on the labeled samples of the *training set*



$$\left\{ \begin{array}{l} \min_{w, b, \xi} \left\{ \frac{1}{2} \|w\|^2 + C \sum_{i=1}^N \xi_i \right\} \\ y_i \cdot (w \cdot x_i + b) + \xi_i - 1 \geq 0, \quad \forall i = 1, \dots, N \\ \xi_i \geq 0, \quad \forall i = 1, \dots, N \end{array} \right.$$

TRansductive Approach: The learning of the classifier is carried out using both *labeled* and *unlabeled* patterns

$$\left\{ \begin{array}{l} \min_{w^{(i)}, b^{(i)}, \xi^{(i)}, \xi^{*(i)}} \left\{ \frac{1}{2} \|w^{(i)}\|^2 + C \sum_{i=1}^n \xi_i^{(i)} + \sum_{j=1}^{\eta^{(i-1)}} C_j^* \xi_j^{*(i)} \right\} \\ y_l^{(i)} \cdot (w^{(i)} \cdot x_l + b^{(i)}) \geq 1 - \xi_l^{(i)}, \quad \forall l = 1, \dots, \eta, \quad x_l \in X^{(i)} \\ y_j^{*(i)} \cdot (w^{(i)} \cdot x_j^* + b^{(i)}) \geq 1 - \xi_j^{*(i)}, \quad \forall j = 1, \dots, \eta^{(i-1)}, \quad x_j^* \in J^{(i)} \\ \xi_l^{(i)}, \xi_j^{*(i)} \geq 0 \end{array} \right.$$

Transductive Support Vector Machines (TSVMs)

- Important issues:

- ✓ **Selection of transductive samples.** Goals:

- i) To select samples with an *expected accurate labeling*;

- ii) To choose *informative samples*.

Iterative selection procedure designed to choose a balanced number of *labeled* and *transductive* samples (unlabeled patterns closest to margin bounds).

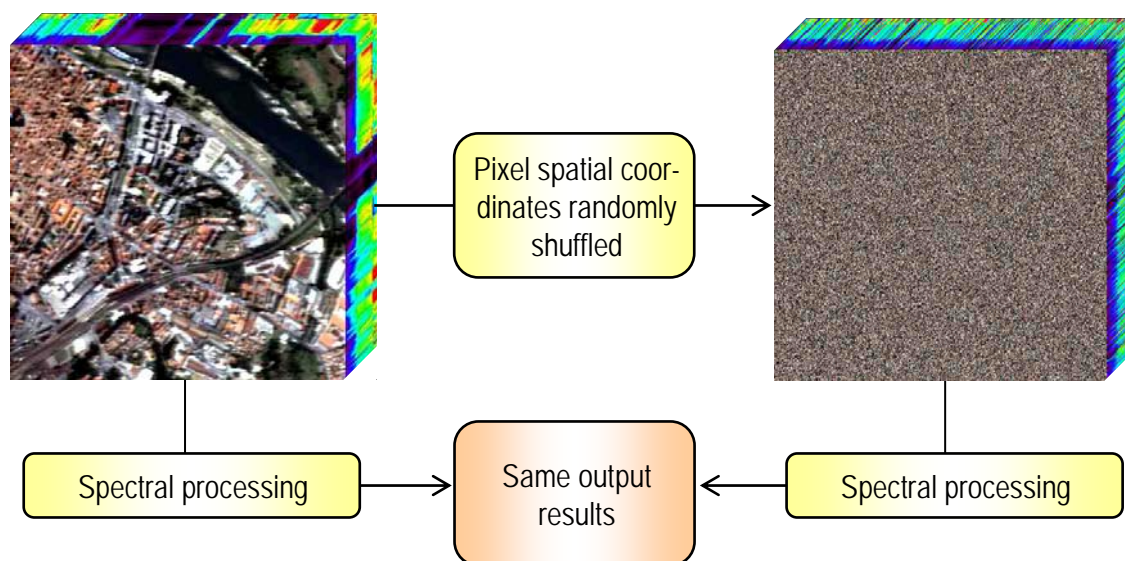
- ✓ **Threshold criterion.** To select transductive samples in a small solution space, a threshold criterion is used to consider the *density* of the selected area. A pairwise labeling strategy is used to alleviate the problem of unbalanced classes.

- ✓ **Regularization parameter.** Used to control the number of misclassified samples that belong to the original training set and the unlabeled set. The larger the regularization parameter, the higher the influence of the associated samples on the selection of the discriminant hyperplane.

- ✓ **Multi-class extension.** As in standard SVMs, the transductive process is based on a structured architecture made up of binary classifiers. It must be possible to give a classification label to all unlabeled samples (*one versus the rest*).

Why integrated spatial/spectral approaches?

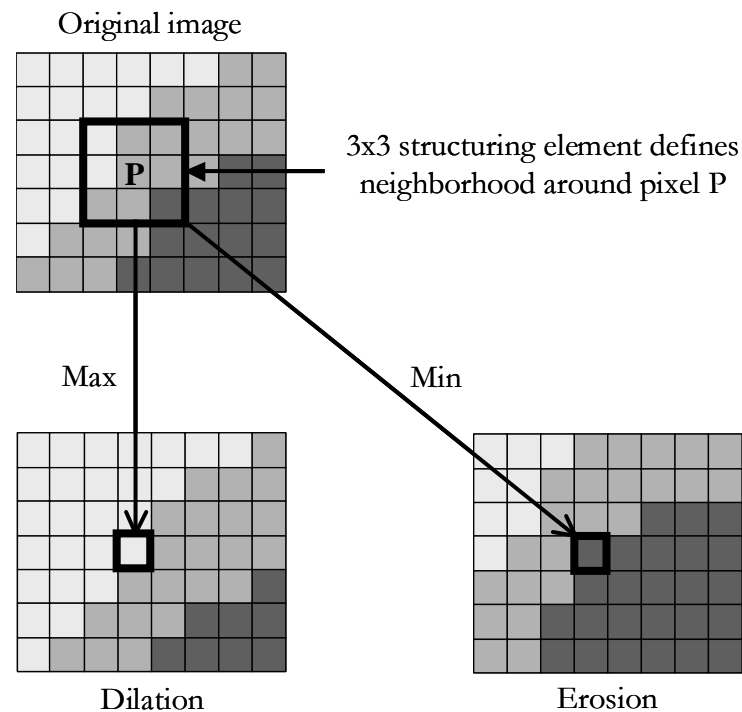
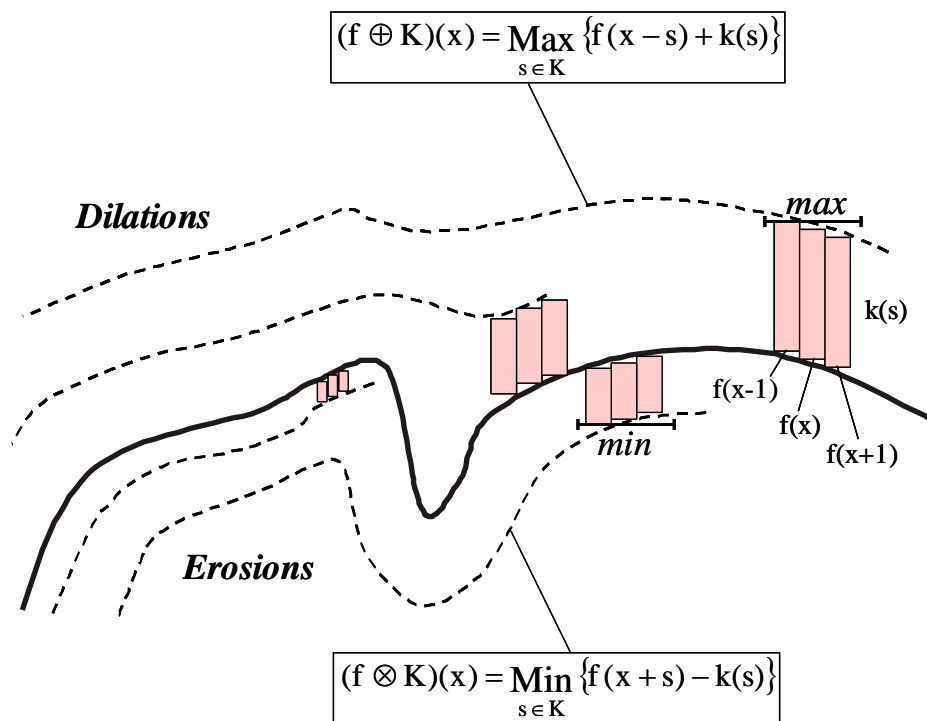
- Much effort has been given to processing hyperspectral image data in *spectral* terms.
- Data analysis is carried out without incorporating information about *spatial* context.



- There is a need to incorporate the *image representation* of the data in the analysis.
- Most available approaches consider spatial and spectral information *separately*.
- Several approaches considered in this work to achieve the desired integration.

Mathematical Morphology

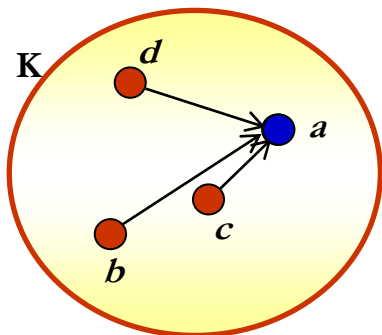
- *Grayscale* morphology relies on a *partial* ordering relation between image pixels.



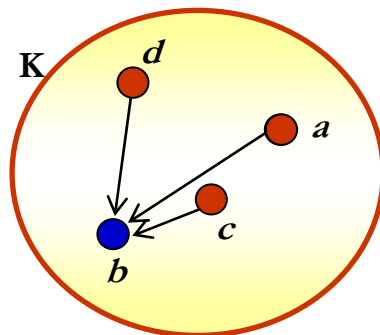
- Morphological operations for *hyperspectral imagery* require *ordering* of image *pixels*.
- Two strategies explored in this work: vector-based ordering and PCA-based ordering.

Vector-based ordering

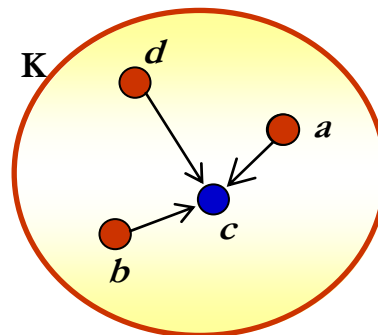
- Based on a *spectral* distance function (SAD, SID) and a *cumulative* distance measure.



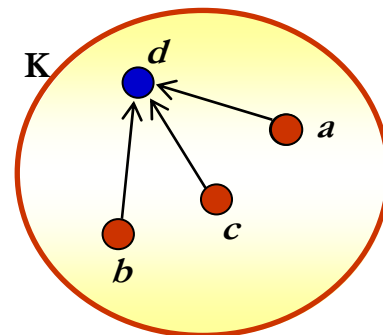
$$D_a = \text{SAD}(b,a) + \text{SAD}(c,a) + \text{SAD}(d,a)$$



$$D_b = \text{SAD}(a,b) + \text{SAD}(c,b) + \text{SAD}(d,b)$$



$$D_c = \text{SAD}(a,c) + \text{SAD}(b,c) + \text{SAD}(d,c)$$

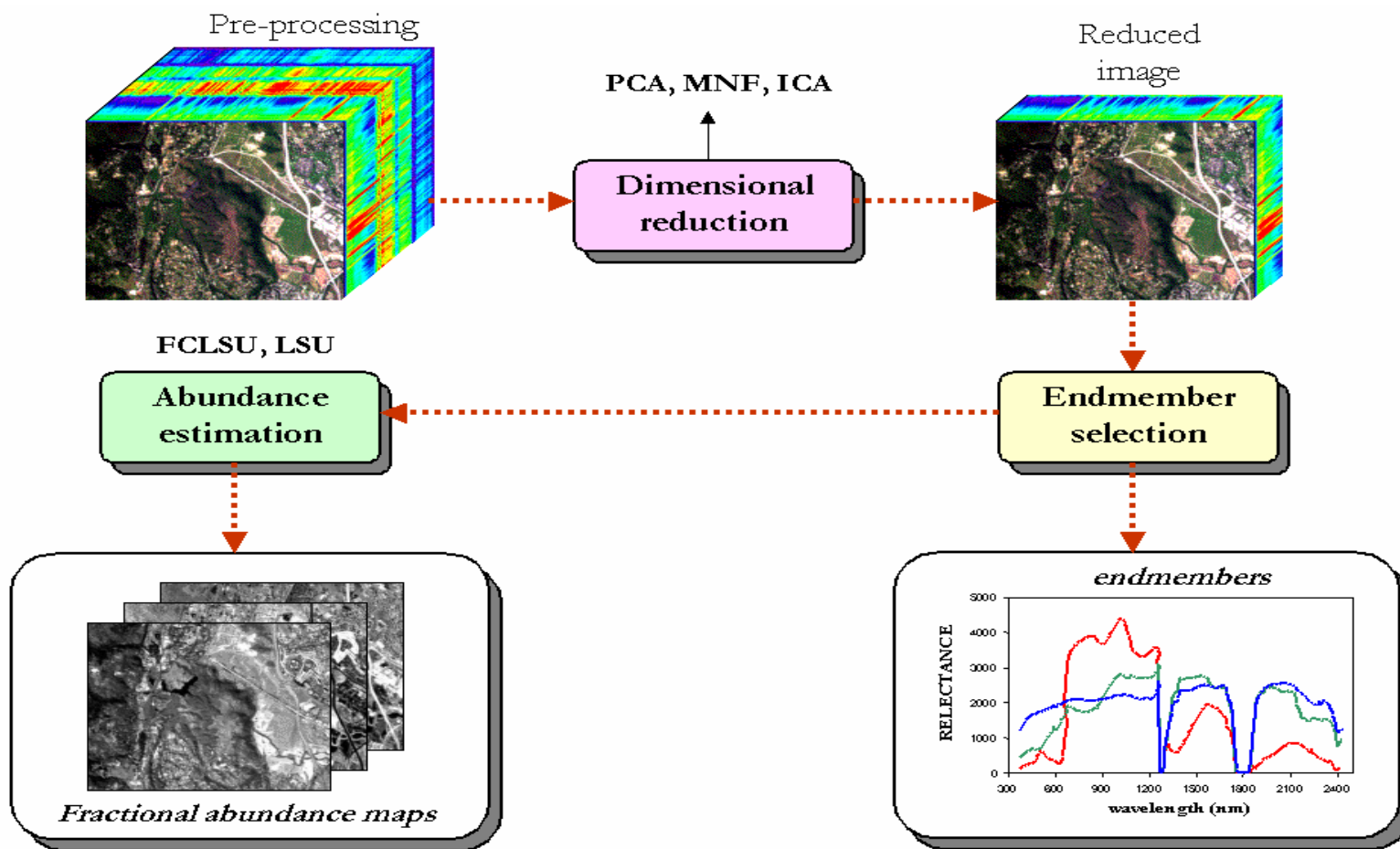


$$D_d = \text{SAD}(a,d) + \text{SAD}(b,d) + \text{SAD}(c,d)$$

- The *greatest* element is the *most spectrally distinct (pure)* in the structuring element.
- The *least* element is the *most spectrally similar (mixed)* in the structuring element.
- Extended dilation* has the effect of expanding pure spectral areas in the image.
- Extended erosion* reduces pure spectral areas and expands mixed areas.
- Particularly suited for spatial/spectral endmember extraction.

Automated Morphological Endmember Extraction.-

- Integration of *spectral* and *spatial* information (computation intensive)
- Selection of the most *spectrally pure* and the *most spectrally* mixed signatures.



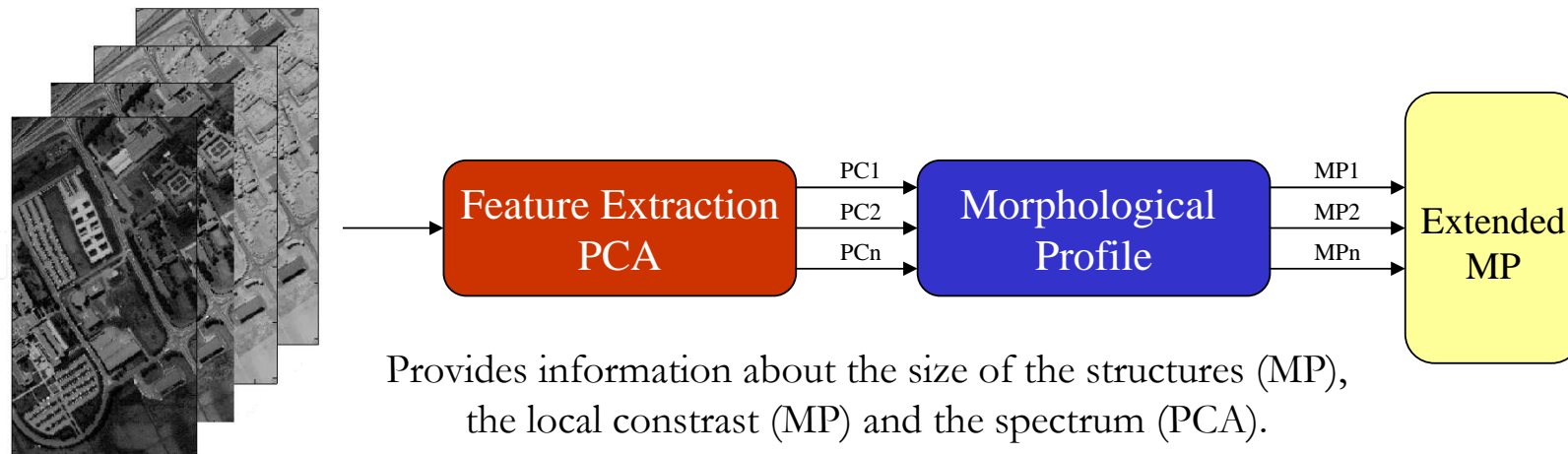
Classification Using Morphological Profiles.-

Uses opening and closing operations to create a *feature vector* for classification:

$$OP_i(x, y) = \gamma_R^{(i)}(x, y), \quad \forall i \in [0, k] \quad CP_i(x, y) = \phi_R^{(i)}(x, y), \quad \forall i \in [0, k]$$

$$MP(x, y) = \{CP_k(x, y), \dots, f(x, y), \dots, OP_k(x, y)\}$$

Extended Morphological Profile.-



$$MP_{ext}(x, y) = \{MP_{PC_1}(x, y), \dots, MP_{PC_k}(x, y)\}$$

Spatial/spectral classification using MRFs

- Minimization of a cost function:

$$U(\mathbf{g}(x, y), C(x, y)) = \alpha U_{spectral}(\mathbf{g}(x, y), C(x, y)) + U_{spatial}(\mathbf{g}(x, y), C(x, y))$$

where $U_{spatial}(\mathbf{g}(x, y), C(x, y)) = \sum_{(i, j) \in G(x, y)} \beta I(C(x, y), C(i, j))$

and $U_{spectral}(\mathbf{g}(x, y), C(x, y)) = \frac{m}{2} \ln |2\pi \Sigma_k| + \frac{1}{2} (\mathbf{g}(x, y) - \mu_k)^T \Sigma_k^{-1} (\mathbf{g}(x, y) - \mu_k)$

SPECTRAL DOMAIN



SPATIAL DOMAIN

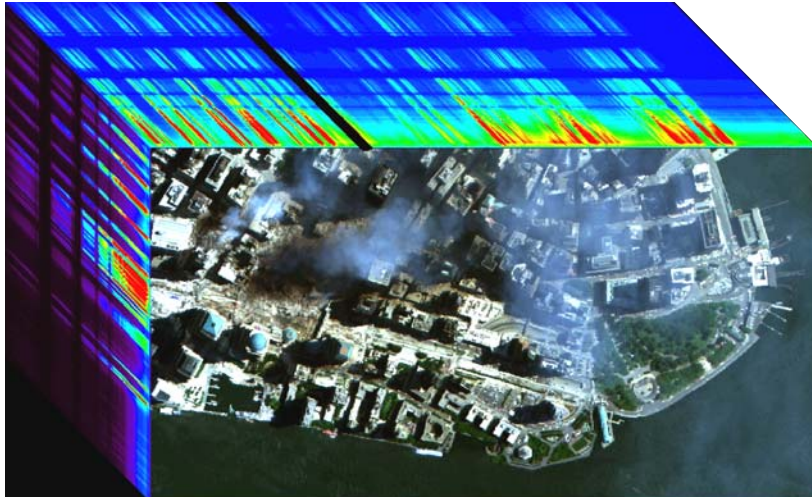


- Integration of the pattern recognition capability of a neuro-fuzzy classifier and the spatial/spectral nature of the probabilistic ML-based MRF framework

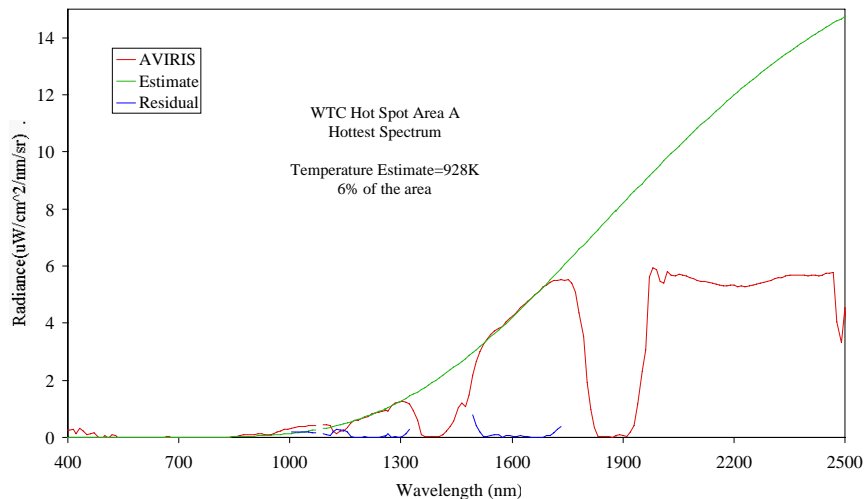
Hierarchical Segmentation (HSEG)

- HSEG produces a set of image segmentations (**segmentation hierarchy**):
 - ✓ *Coarser* segmentations produced from merges of regions from *finer* segmentations.
 - ✓ Region boundaries maintained at the full image spatial resolution.
- HSEG is a hybridization of Hierarchical Step-Wise Optimization (region growing) with **spectral clustering**, controlled by *spclust_wght* (an input parameter).
- A recursive approximation of HSEG, called RHSEG, is much more computationally efficient (especially for *spclust_wght* > 0.0):
 - RHSEG **recursively** subdivides the image data and then recombines the results such that the number of regions handled at any point in the program is restrained.
 - The recombination step of RHSEG requires special blending code to avoid **processing window artifacts**.

Why High-Performance Computing is Crucial?



Fire Temperatures



Biomass Burning: Sub-pixel temperatures and extent, smoke, combustion products...

Environmental Hazards: Contaminants (direct and indirect), geological substrate...

Coastal and Inland Waters: Chemical and biological standoff detection, oil spill monitoring and tracking...

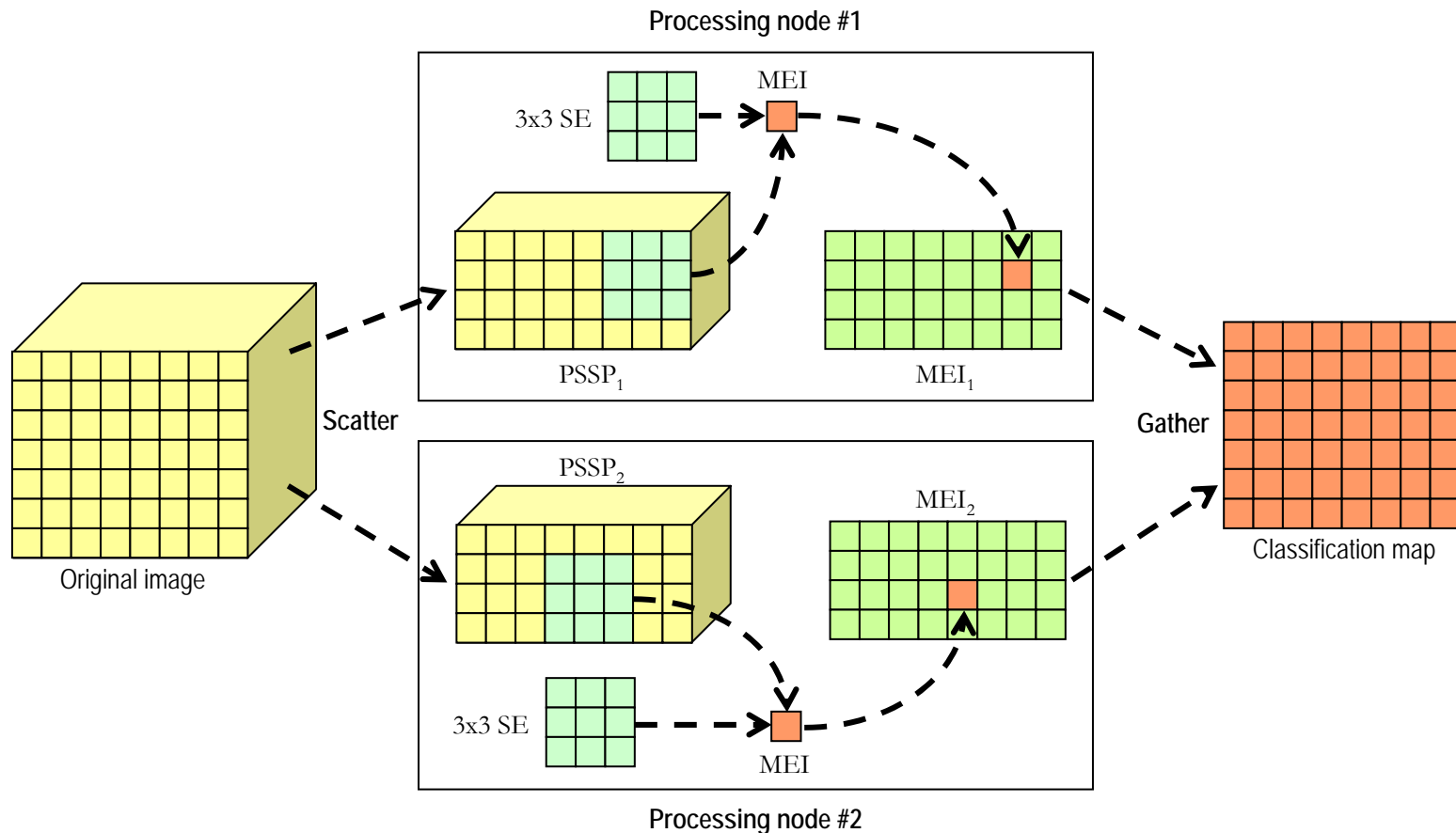
Ecology: Chlorophyll, leaf water, lignin, cellulose, pigments, structure, nonphotosynthetic constituents...

Commercial Applications: Mineral exploration, agriculture and forest status...

Military Applications: Detection of land mines, tracking of targets, decoys...

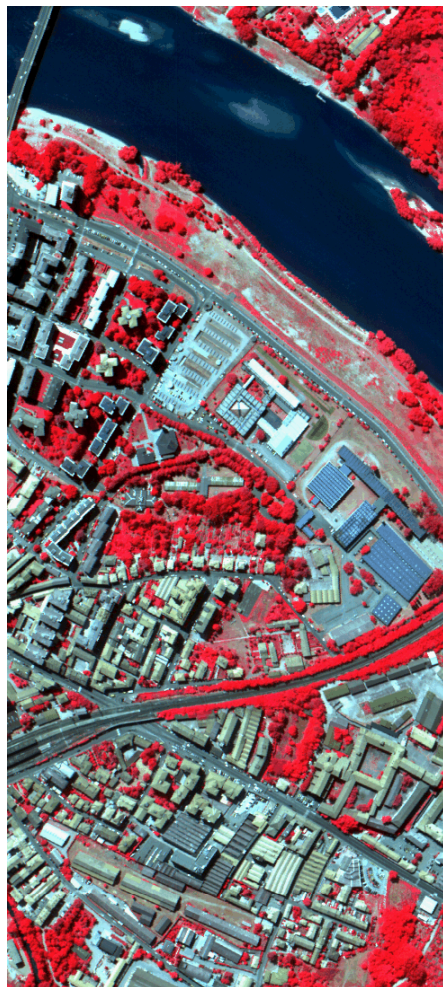
Others: Human infrastructure, medical...

Parallel Framework for Morphological Methods



- The *master* processor is in charge of distributing the work among the *workers*.
- Each partition is processed *independently*, and the master gathers the final result.

ROSIS Urban Hyperspectral Data Over Pavia, Italy

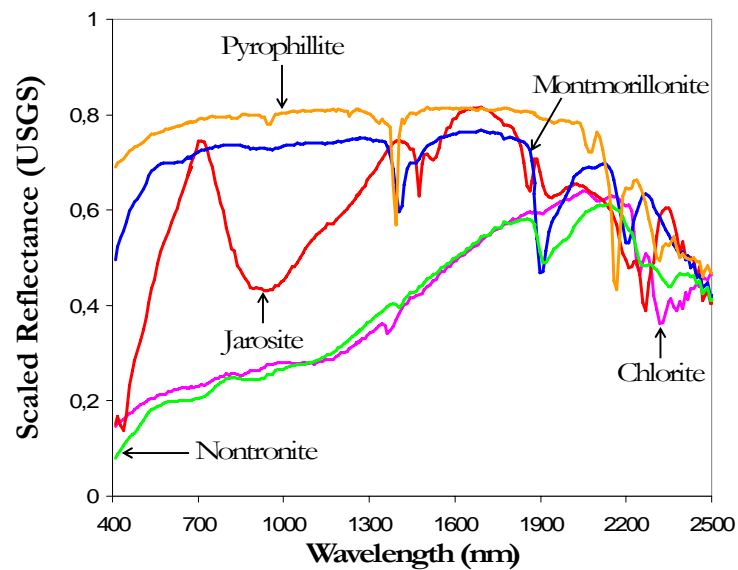
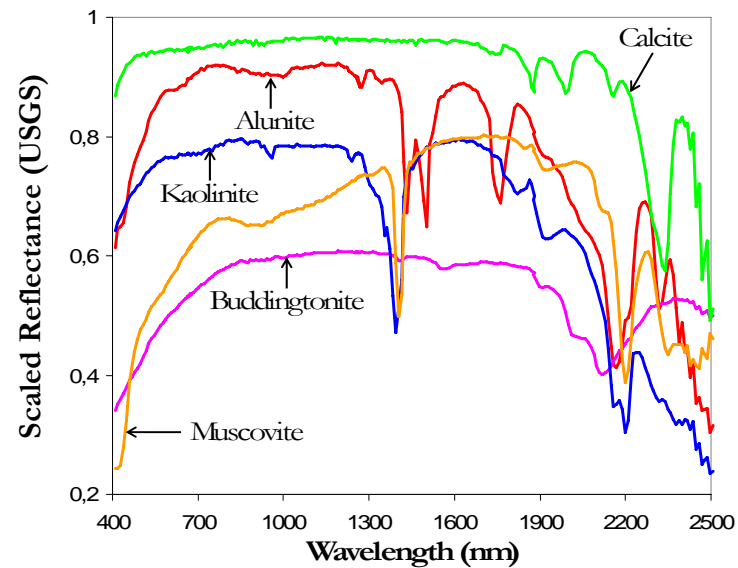


Subset #1

Subset #2

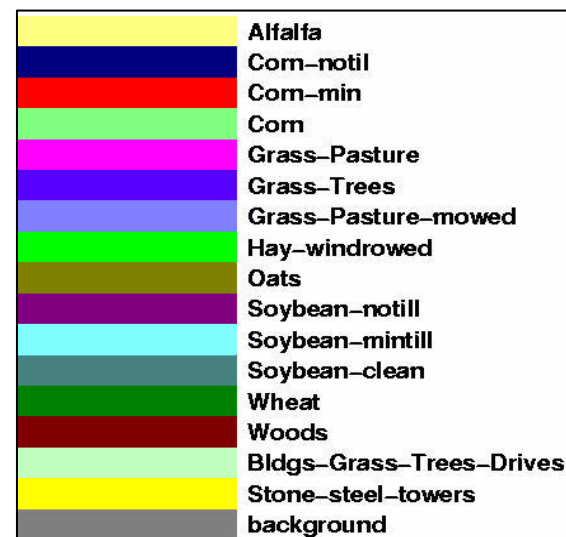
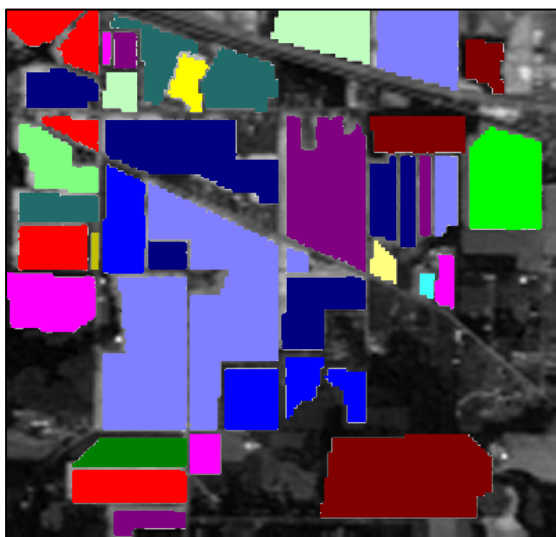
Subset #3

AVIRIS Data Over Cuprite, Nevada



Standard SVMs vs Transductive SVMs.-

- Tested using AVIRIS data over Indian Pines, made up of 16 ground-truth classes (7 classes were discarded due to insufficient training samples).
- Gaussian RBF classifier and *one versus the rest* architecture with 9 binary classifiers.



Percentage of Training Samples	Number of Samples	Overall Accuracy		Kappa	
		SVMs	Proposed TSVMs	SVMs	Proposed TSVMs
5%	237	73.41	76.20	0.68	0.71
10%	475	76.46	80.21	0.73	0.77
25%	1189	82.17	84.83	0.79	0.82

Composite Kernel-Based Image Classification.-

- Excellent results on a wide range of scenarios (tested on all 16 Indian Pines classes)

	Overall accuracy	Kappa
Spectral classifiers[†]		
Euclidean (Tadjudin and Landgrebe, 1998)	<u>48.23</u>	—
bLOOC+DAFE+ECHO (Tadjudin and Landgrebe, 1998)	<u>82.91</u>	—
k_ω (Gualtieri, 1999)	<u>87.30</u>	—
k_ω (developed in this paper)	<u>88.55</u>	0.87
Spatial/spectral classifiers		
<i>Mean</i>		
Spatial	<u>84.55</u>	0.82
Stacked	94.21	0.93
Summation	92.61	0.91
Weighted	95.97	0.94
Cross-terms	94.80	0.94
Summation + Stacked	95.20	0.94
Cross-terms + Stacked	95.10	0.94
<i>Mean and standard deviation[‡]</i>		
Spatial	<u>88.00</u>	0.86
Stacked	94.21	0.93
Summation	95.45	0.95
Weighted	96.53	0.96
Summation + Stacked	96.20	0.95

TrueMap



Spectral SVM



Weighted Kernel



- More advanced contextual/textural extractions can be easily integrated.
- Extensions to *multi-temporal* and *semi-supervised* versions yield good results.

Subset #1 ROSIS Urban Data



FUZZY ARTMAP



DAFE/MRF

	DAFE/MRF	Neuro-fuzzy
Overall accuracy	97.27	97.29
Water	99.04	99.71
Trees	91.27	93.19
Grass	97.09	94.80
Parking lot	76.83	71.99
Bare soil	93.33	93.36
Asphalt	99.65	81.87
Bitumen	88.45	96.42
Tiles	98.33	99.98
Shadow	99.86	99.93

- Similar classification accuracies
- Different performances in border areas

- The DAFE/MRF framework achieves better geometrical characterization of buildings and roads.
- The neuro-fuzzy procedure performs better in homogeneous areas.

Extended Morphological Profiles vs Spectral Info.-

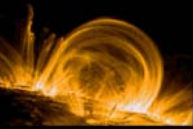
- PCA was applied to the original spectral information, and the first *three* principal components were retained (99% of the *cumulative variance*).
- Morphological profiles were constructed *for each component*, based on 10 opening/closings by reconstruction and a disk-shaped structuring element.
- Classification results using 102 *spectral bands* vs. 63 *morphological features*:

	Original spectral information	Extended morphological profile
Overall accuracy	80.99	85.22
Average accuracy	88.28	90.76
Kappa	76.16	80.86
Asphalt	83.71	95.36
Meadow	70.25	80.33
Gravel	70.32	87.61
Tree	97.81	98.37
Metal Sheet	99.41	99.48
Bare Soil	92.25	63.72
Bitumen	81.58	98.87
Brick	92.59	95.41
Shadow	96.62	97.68

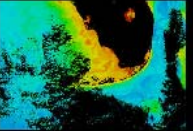
Thunderhead (NASA)

<http://thunderhead.gsfc.nasa.gov>


Aggregate Specification	
Number of nodes	256
Total processors	512
Total memory (Gb)	256
Total disk (GB)	20480
Interconnect 1	Myrinet 2000
Interconnect 2	Gigabit Ethernet
Total peak performance (Gflops)	2457.6
Node Specification	
Motherboard	Tyan Thunder 2720
Number of processors	Dual Intel 4 Xeon 2.4Ghz
Memory (Gb)	1
Local disk (Gb)	80
Interconnect 1	Myrinet 2000
Interconnect 2	Gigabit 10/100/1000
Peak performance (Gflops)	9.6



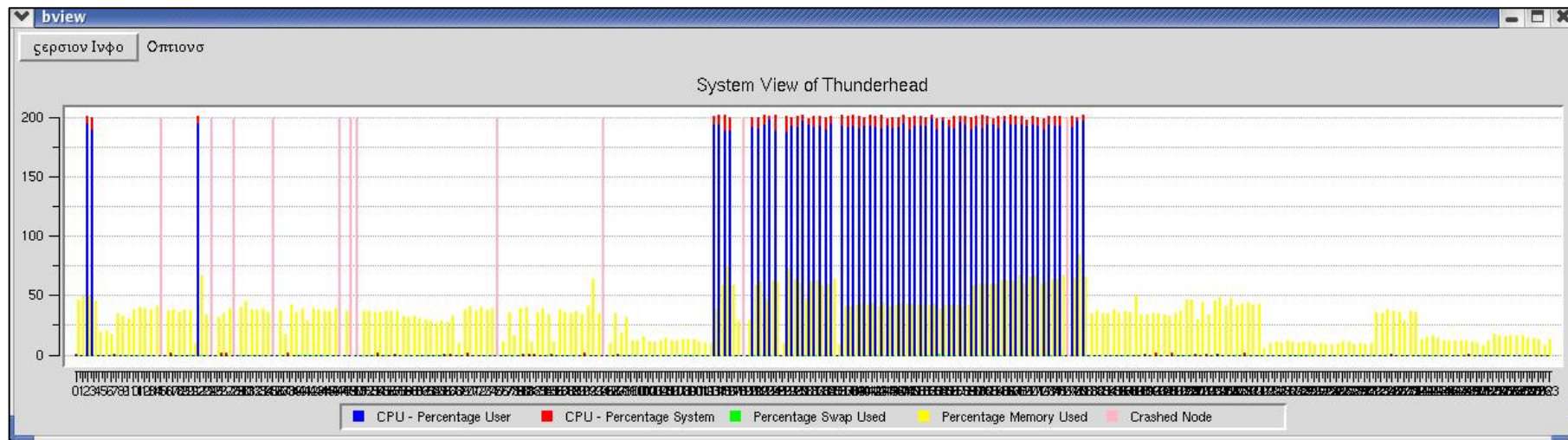
NASA/Goddard Space Flight Center
High Performance Computing



HYDRA Cluster:
Thunderhead, Medusa,
Orka, Pivot, BBBLUE

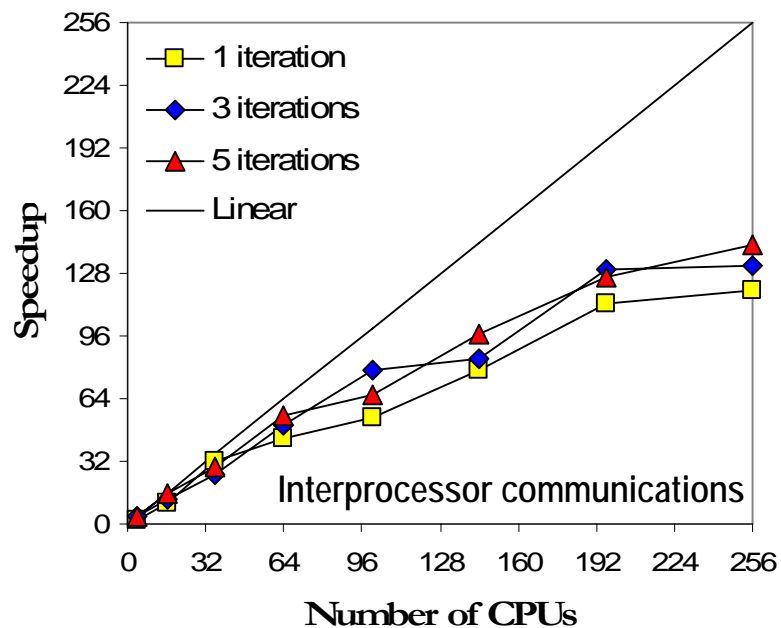
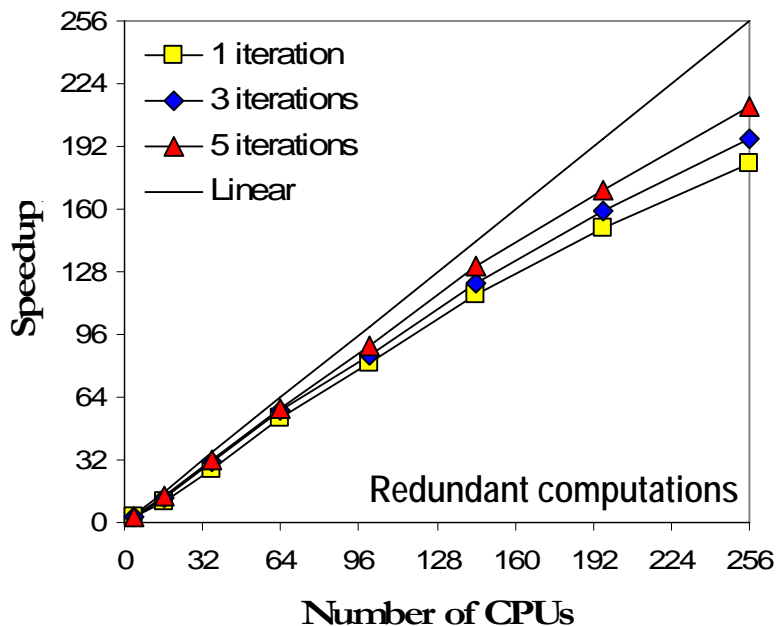


NASA Summer School for High Performance Computing:



Performance of Morphological Endmember Extraction.-

- Algorithms were implemented in C++ using calls to Message Passing Interface (MPI).
- Using redundant computations versus communications was crucial:



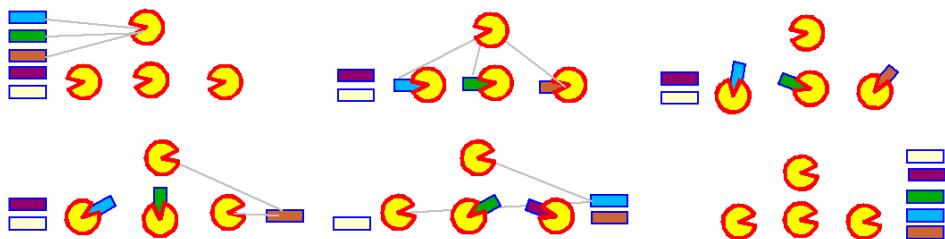
Processing times (seconds) for different numbers of processors on Thunderhead (AVIRIS Cuprite)

	1	4	16	36	64	100	144	196	256
Redundant	9452+13	4075+10	917+12	381+11	205+15	128+16	89+14	65+11	50+10
Interprocessor	9356+143	4062+151	889+160	371+194	205+225	124+243	83+261	62+268	49+292

A. Plaza et al., "A quantitative and comparative analysis of endmember extraction algorithms," *IEEE-TGARS* (42), 3, 650-663, 2004

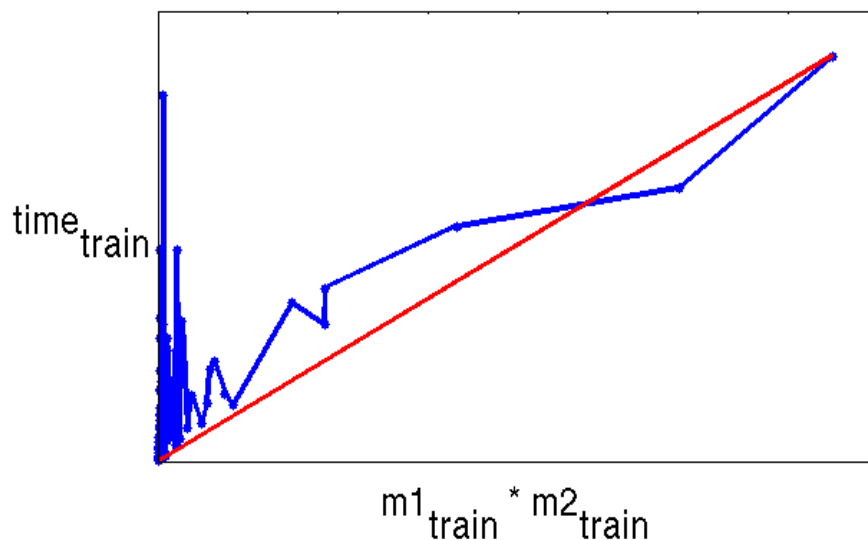
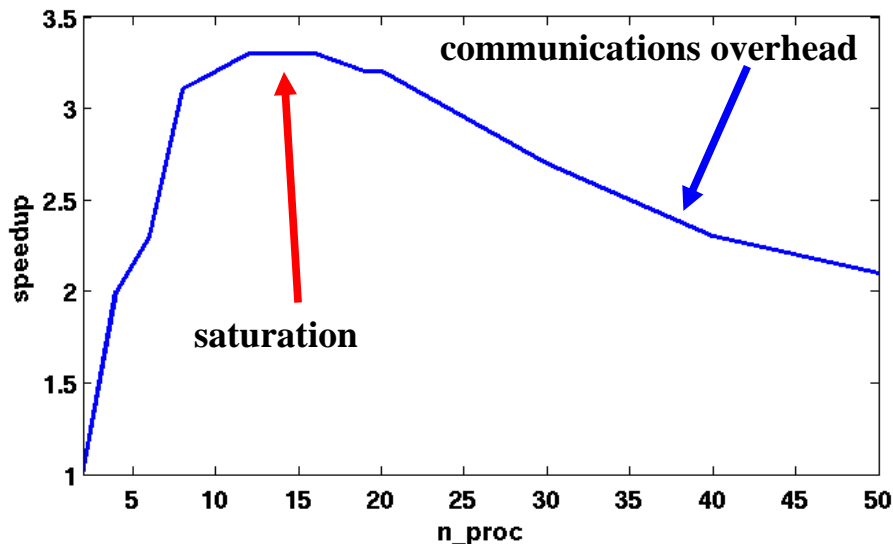
Performance of Parallel Support Vector Machines

MPI Code to Implement *boss_workers*:



Processors are *asynchronous* (not in lockstep): Who finishes first is non-deterministic. Boss processor keeps track, $n_proc - 1$ workers do the work. If all sub-tasks take the same time, then speedup is linear for $n_tasks < n_proc - 1$. However..

Results for Indian Pines Data 16 classes: 145 x 145 pixels 200 bands/pixels => build 120 pair classifiers: 120 training tasks + 120 testing tasks + 1 voting task (could have done training+testing as a single task)



Performance of Recursive Hierarchical Segmentation (RHSEG).-

- Key concern: selecting an appropriate dissimilarity function.
- Currently available functions: 1-norm, 2-norm, inf-norm, BSMSE, BMMSE.
- Parameter *spclust_wght* gives a lot of flexibility for the integration of spatial/spectral info.

1-Norm	2-Norm	∞ -Norm	BSMSE	BMMSE
91.5	90.5	89.1	90.5	89.1

Impact of dissimilarity function on classification of Subset #3
(Region means modeled as the mean of each ground-truth class)

<i>spclust_wght</i> = 1.0	<i>spclust_wght</i> = 0.5	<i>spclust_wght</i> = 0.1
90.5 (9 regions)	96.5 (14 regions)	97.7 (18 regions)

Impact of *spclust_wght* on classification of Subset #3
(Region means were initialized using the ground-truth data)

Processing times (seconds) for parallel RHSEG executed on Thunderhead (Subset #3 or ROSIS data)


	1	4	16	64	256
Time	2061	568	155	48	25
Speedup	1.0	3.6	13.3	49.9	82.4



<http://tco.gsfc.nasa.gov/RHSEG/index.html>

Conclusions

- The introduction of the concept of imaging spectroscopy by Alex Goetz established the foundations a field which is still emerging in the design of data processing techniques.
- The special characteristics of hyperspectral images pose *new processing problems*, not found in other types of remote sensing data.
- Kernel methods offer an interesting solution to deal with the *high-dimensional nature* of the data and the *limited availability of training samples* (supervised classification).
- The *integration of spatial and spectral information* allows for the development of enhanced supervised/unsupervised analysis techniques.
- Most of the algorithms discussed in this work are dominated by regular computations (appealing for the design of *parallel implementations*).
- Techniques developed in this work show the increasing sophistication of a field that is rapidly maturing at the intersection of many different disciplines.



Advanced Processing of Hyperspectral Images

State of Science of Environmental Applications of Imaging Spectroscopy
in honor of Dr. Alexander F.H. Goetz

A. Plaza¹, J. A. Benediktsson², J. Boardman³, J. Brazile⁴, L. Bruzzone⁵, G. Camps-Valls⁶,
J. Chanussot⁷, M. Fauvel^{2,7}, P. Gamba⁸, A. Gualtieri^{9,10}, M. Marconcini⁵, J. C. Tilton⁹, G. Trianni⁸

¹Univ. Extremadura (Spain), ²University of Iceland, ³Analytical Imaging and Geophysics LLC (USA),

⁴Univ. Zürich (Switzerland), ⁵Univ. Trento (Italy), ⁶Univ. Valencia (Spain), ⁷INPG Grenoble (France),

⁸Univ. Pavia (Italy), ⁹NASA/Goddard Space Flight Center (USA), ¹⁰Global Science & Technology (USA)